Egyptian Journal of Chemistry

http://ejchem.journals.ekb.eg/

Predicting the Removal Amount of Aqueous Thiocyanate Anions by Titanium Dioxide Nanoparticles Using Novel Artificial Neural Network Methods

Rashin Andayesh[1,2]*, Mehran Zargaran[1,2]

[1] *Department of Chemistry, Science and research Branch, Islamic Azad University, Ahvaz, Iran*

[2] *Department of Chemistry, Islamic Azad University of Ahvaz, Ahvaz, Iran*

In this work, the adsorbent method is performed using artificial neural network (ANN) modeling. The adsorbent is applied for removal of Thiocyanate in water samples using Titanium Dioxide (TiO2) nanoparticles as effective sorbent. Prediction amount of Thiocyanate removal was investigated with novel algorithms of neural network. For this purpose, six parameters were chosen as training input data of neural network functions including pH, time of stirring, the mass of adsorbent, volume of TiO2, volume of Fe (III), and volume of buffer. Performances of the suggested methods were examined using statistical parameters and found that it is an efficient, effective modeling satisfactory outputs. The radial basis function (RBF) and Levenberg-Marquardt (LM) algorithm could accurately predict the experimental data with correlation coefficient of 0.997939 and 0.99931, respectively. The Pearson's Chi–square measure was found to be 29.00 for most variables, indicating that these variables are likely to be dependent in some way.

Key words: Thiocyanate, Titanium Dioxide Nanoparticles, Fe-SCN complex, Artificial Neural Network, Pearson's Chi–square

Introduction

In biomedical fluids, determination of Thiocyanate is associated with biomedical and toxicology [1-3]. These compounds would cause some serious effects, especially on the Nervous system, including Alzheimer's disease, nervousness, hallucination, psychosis, delusion, and seizure [4]. Negative effects of this substance decrease by increasing the molecular mass of Thiocyanate alkyl [5]. This substance is found in industrial waste-water, pesticide residues, and organic metabolism. Thiocyanate is released as the main product of detoxification and reforming of Hydrogen Cyanide. It is synthesized from a connection between existing sulfur molecules such as thiosulfate and cyanide and, eventually, is catalysed by Rodz enzymes [6,7]. These particles exist in all eatable plants, water solutions, urine,

saliva, and human plasma [8]. So, there is always conjunction between cyanide in blood, Thiocyanate in plasma, and Thiocyanate in saliva. This anion distributes its negative charge between sulfur and nitrogen almost the same. As a result, it can be treated as a nucleophile such that two or three metal can join to it. The anion also connects to Thiocyanate from N side if the metal is a hard acid and connects from S side if it is a soft acid [9]. The first study concerning the determination of Thiocyanate particles in biological fluids was conducted based on spectrophotometric detection and intricacy of colors [10].

Some methods frequently applied for the removal of metals are precipitate [11], ion exchange [12], severe filtrations [13], adsorptions [14,15], membrane separation [16], and constructed wetlands [17]. In comparison with

other methods, adsorption often can be considered as a superior particle removal method because of its cost-effective, easy setup, flexibility and high efficiency [18]. Researchers are more interested in nano-sorbents because of their sorbent particle size and surface treatment, which causes the high chemical reactivity and increases the interference between absorption and adsorption material [19,20]. The concentration range of nano-sorbents is 1-1000 ppm owing to the removal of pollutants [21]. During recent years, different studies have been done for removing Thiocyanate. TiO_2, is also known as Titanium Oxide (IV) or Titania, White Titanium, and White Pigment when used as a pigment. All properties of TiO_2 exist in nano-TiO_2 just, except that its particles are very smaller, which leads to its additional extraordinary properties. It has a larger surface and a higher efficiency owing to its smaller particle sizes. Two important properties of this substance that make it so efficient and useful are being auto-cleaner and photo-catalytic.

When the size of TiO_2 particles, decreases to nano-scale, the photo-catalytic activity can increase due to the increase in the effective surface. TiO_2 is used to remove organic pollutants such as Toluene, surfactants, insecticides, aromatic sulfides, hydrocarbons, and organic dies [22]. This oxide usually is used as a reliable substance for eliminating some detrimental particles, especially in environmental usages [23]. Some of the merits of TiO_2 include being a suitable adsorbent, chemical and physical stability, nontoxic, resistance to rusting, and economical justification [24].

Unlike most researches which use photocatalytic methods, in this study, the mechanism of removal of Thiocyanate with TiO_2 is based on a reversible physical adsorption. In this method, the adsorbed Thiocyanate can be easily extracted from adsorbent and there is no need to use a modifier to adjust the surface of the nanoparticles. Furthermore, nanoparticles can be used several times which in turn, shows the high performance of the method. Modeling the removal process allows evaluating the influence of every parameter and simulation of the removal efficiency with a lower number of experiments. In this regard, random forest (RF), adaptive Neuro-fuzzy inference system (ANFIS), least squares support vector machines (LS-SVM), and artificial neural network (ANN) as some intelligent models are efficient for predicting the adsorption process

[25,26]. ANN represents a promising modeling technique, especially for data sets having non-linear relationships. It requires no knowledge of the data source and can combine and incorporate both literature-based and experimental data to solve problems. In this study, the capability of artificial neural network (ANN) was investigated for predicting metal ions removal. In this regard, ANN was compared with the experimental data to determine the relationship of six input parameters on Thiocyanate adsorption capacities: pH, time of stirring, the mass of sorbent, volume, and concentration of TiO_2, and volume of Fe (III) [27]. The novelty of the present study is using neural network functions in anticipating the removal of Thiocyanate in the prepared water samples. The available neural network algorithms predict removal percentage values instead of doing all of the required experiments. Reducing the cost of raw materials and reducing the use of expensive laboratory equipment and instruments are among the advantages of this method. Also, it can lead to less time needed for the analysis and conclusions. In the present study, the ability of radial basis function and multi-layer perceptron algorithms are assessed to predict the amount of removed Thiocyanate and, eventually, the performance of the neural network method is tested by the valid statistical criteria. Two algorithms, including multilayer perceptron (MLP) and radial basis function (RBF) were used to evaluate the performance of method. The results showed that two models satisfactorily predicted the adsorbed amount of Thiocyanate from wastewater [28].

Experimental

Material and methods

Solid Iron (III) Chloride (purity = 99), solid Potassium Thiocyanate (purity= 99-100), solid Sodium hydroxide (purity= 99-100) and other materials with a high purity were supplied from Merck Company (Germany). TiO_2 adsorbent (purity = 99.5-100) was purchased from Neutrino local company.

For two beam spectrophotometer, model Lambda 135 (manufactured by Perkin-Elmer) was used. In addition, a 1cm TB glass was applied for the adsorption of the Iron-Thiocyanate color complex in λ = 456.8 nm and drew a spectrum. pH meter model F-11 (manufactured by Horiba Company, Japan) was used for pH control in aqueous solutions. Weight measurements were done using

a balance (model BP210D, weight capacity = 200 g, and precision = 0.0001) manufactured by Sartorius company in Switzerland. Pyrex glass containers such as a volumetric flask, bécher, pipette, Erlenmeyer flask, and glass stirrer were used. A centrifuge H-11n (manufactured by Kokusan Company, Japan) was used for the centrifuging the synthesized particles. For taking transmission electron microscopy (TEM) photos, a Leo 906 device manufactured by Germany was applied. A syringe filter manufactured by the Chinese Biofil Company (pore size = 0.22 μm and maximum bear the pressure = 4.5 bar and as a disposable) was also used during the experiments.

Preparation of samples for analysis

Iron (III) solution (0.1 molL^{-1})

First, using a digital balance, 2.70 g of Iron (III) chloride hexahydrate was carefully weighed and was transferred to a 100 ml volumetric flask. Next, it was solved in a small amount of water and was brought to volume by adding fresh distilled water.

Thiocyanate solution (1000 μg.ml^{-1})

Using a digital balance, 0.169 g of solid Potassium Thiocyanate was carefully weighed and transferred to a 100 ml volumetric flask. It was solved in a small amount of water and was brought to volume by adding fresh distilled water.

Ammonia buffer solution (0.02 molL^{-1})

Using a micropipette, 0.75 ml of 13.38 M ammonia solution (0.91 g.ml^{-1}, 25% W/W) was transferred in a 500 ml volumetric flask and was brought to volume. The pH of the solution was adjusted by 0.1 M hydrochloric acid solution.

Hydrochloric acid solution (0.1 molL^{-1})

About 8.33 ml of 12 M hydrochloric acid solution (1.19 g.ml^{-1}, 37%W/W) was poured in a 1000 ml volumetric flask. Thus, it was brought to 1 L of volume by adding distilled water.

Sodium hydroxide solution (0.1 molL^{-1})

According to calculations and to synthesize sodium hydroxide solution with a concentration of 0.1 molL^{-1}, 1.00 g solid sodium hydroxide with high purity was weighed. Then, after solving in a small amount of water, in a 250 ml volumetric flask, it was brought to volume by adding distilled water.

General procedure

To adsorb and remove the Thiocyanate by TiO$_2$ nanoparticles, 1 ml of 100 μg.ml^{-1} Thiocyanate solution, 1 ml of 0.1 M Iron (III) solution, and 0.5 ml buffer (pH = 9) were spilled in a 10 ml volumetric flask and was brought to volume by adding distilled water. The resulting solution was transferred to a 50 ml bécher containing 0.5 g of TiO$_2$ nanoparticles. Thus, the mixture was placed on a magnetic stirrer for about 15 minutes and nanoparticles were removed by using a filter.

Artificial neural network

The effect of operating conditions on the removal process is often non-linear, which leads to additional problems for developing and solving the outcome using non-linear theoretical models. Therefore, using theoretical models and multiple linear regression (MLR) is necessary [29]. During the module design, the relationship between different modules is regarded. Artificial neural network (ANN) is one of the most powerful tools to reach this purpose. This method can introduce mathematical functions for linear and non-linear systems. Many studies have proposed ANNs for solving nonlinear problems. An accurate trained ANN can usually provide better performance in comparison with conventional modeling methods [30,31]. This method is widely used in various research areas for acquiring experimental information for designing water treatment model [32,33]. In this study, the input parameters were variables affecting the cyanide removal, including pH (over range of 4-10), time of stirring (over range of 1-20 min), the mass of sorbent (over range of 0.1-0.6 g), volume (over range of 1-50 ml), and concentration of TiO$_2$ (over range of 10-200 mg.ml^{-1}), and volume of Fe (III) (over range of 0.005-0.020) and the output parameter or the target parameter was cyanide removal efficiency and the network works based on the correspondence between the input and target. Fig.1 shows how the ANN deals with these data.

Radial basis function

The radial basis function (RBF) network is one of the most popular ANNs. These networks have the best performance when there are a large number of training data. There are three types of layers in its structure that play different roles. The input layer connects the network to the control variables. The newrb function adds neurons into the hidden

layer of the radial basis network up to the time that the amount of data mean square error is close to the target or the number of determined neurons is finished. The output layer is a linear layer that leads to a response from the network that creates an active pattern on the input layer. Neurons in different layers are connected to each other by the weight and bias. If C is the measured value in testing and C_0 is the initial value of the desired parameter, the output vector of the j-th neurons of the hidden layer and the k-th neurons of the output layer are calculated by the Equation (1) [34].

$$Y_k = \sum_{k=1}^{N} W_{kj} Y_j + W_{k0} = \sum_{k=1}^{N} W_{kj} \, exp\left[-0.8326^2 \times \left[\frac{\|W_{ji} - x_i\|}{C_i}\right]^2\right] + W_{k0} \qquad \text{Eq. (1)}$$

Where W_{kj} is the output of the hidden layer weights and W_{ji} is the input of the hidden neurons weights, C_i is 0.8326/ spread. Y_j shows the j-th output vector of the hidden layer; Y_k is the k-th output vector of the output layer; X_i is the i-th input vector; N is the number of output neurons; and n denotes the number of neurons of the hidden layer (Fig.2). The proposed RBF model was designed and taught by Matlab software with newrb function. The newrb function adds neurons into the hidden layer of the radial basis network up to the time that the amount of data mean square error is close to the target or the number of determined neurons finish. This function is made of two-layer networking. The first layer has radbas neurons and the second layer contains purelin neurons that adjust the weights are calculated to create an appropriate network.

Levenberg-Marquardt function

Levenberg-Marquardt (LM) algorithm in a multilayer perceptron (MLP) can be regarded as an effective and efficient nonparametric technique for estimating the unknown parameters. The first layer is called the input layer and includes a number of neurons often equal to the number of inputs. In general, each input is connected to all other inputs. Hidden layers are all layers between the input and output layers and include a vast number of neurons. Generally, a trained MLP has very satisfactory generalized capability to map input patterns into target estimation. The theoretical framework of MLP modeling is discussed in detail in [35,36]. The LM algorithm provides a solution for minimizing the nonlinear least squares. The function that should be minimized is expressed by Equation (2) to (4) and defined by train lm function in Matlab software [37].

$$f(x) = \frac{1}{2} \sum_{j=1}^{m} r_j^2(x) \qquad \text{Eq. (2)}$$

$$r(x) = (r_1(x), r_2(x), \ldots, r_m(x)) \qquad \text{Eq. (3)}$$

$$f(x) = \frac{1}{2} \|r^2(x)\|^2 \qquad \text{Eq. (4)}$$

Despite the structural similarities between the two MLP and RBF methods, RBF needs to have more neurons compared with back-propagation networks, nevertheless, they took advantage of their shorter design time compared to standard MLP networks. For this reason, the rate of learning and training for RBF networks is faster.

Methodology

RBF and MLP algorithms were used to develop the removal method. The data were divided into two categories including training and testing. These data consist of 40 rows and 6 columns related to parameters effective in the removal process. A total of 32 rows of data were selected randomly as training data and 8 rows for the training purpose. The efficiency of the neural network was evaluated using several statistical parameters such as root mean square error (RMSE), the mean absolute error (MAE), and the coefficient efficiency (CE). The more the uncertainty, mean absolute error, and standard error of the studied parameters are closer to 0, the higher the performance of the designed ANN for predicting the test data would be. For a suitable algorithm of the neural network, the coefficient of determination is close to 1 and has a range between 0 and 1. If this parameter is 1, there will be a perfect correlation between measured and predicted data. On the other hand, if the coefficient of determination is 0, the regression equation cannot predict the desired values by no means.

Results and discussion

Artificial neural network modelling

The experimental data obtained from the experimental observations are divided into training and testing sets. The data set consists of 40 input values. From these 32 data sets are used for training and the remaining is used for testing the network. Then, the performance of the network was studied using different statistical performance parameters such as MAE, RMSE and CE values. The train data and test data are shown in Table 1 and Table 2, respectively.

Experimental   parameters   of   Thiocyanate adsorption

Effect of pH

Variation of pH value in the range of 4 to 10 was done with the 1 ml of 1000 mg L^{-1} Thiocyanate solution was added to 50 ml volumetric flasks. Different amounts of sodium hydroxide and hydrochloric acid were added to prepare solutions with pH in the range of 4 to 10. 5 ml of 0.1 M Fe (III) solution was added to each solution and was brought to volume by adding distilled water. After that, each solution was moved to a bécher and placed in contact with Titanium dioxide nanoparticles. Then, each bécher was stirred for 20 min. Next, the adsorption of each solution was determined by spectrophotometry at $\lambda = 456.8$ nm after clearing by syringe filter and, the maximum adsorption obtained at pH = 9, thus this pH was chosen as optimum pH. The agreement between the ANN model predictions and the experimental data as a function of initial pH is shown in Fig.3.

Effect of the buffer

0.5 ml of ammonia buffer with 0.02 M concentration was determined as the optimal amount of buffer because the ammonia buffer can destroy the adsorption spectrum and decline λ_{max} in volumes more than 0.5 ml and concentrations greater than 0.02 M. This amount of buffer was added to 1 ml of 0.1 M Fe (III) solution and 1 ml of 100 µg.ml^{-1} Thiocyanate solution at pH = 9. Next, it was brought to 10 ml volume by adding distilled water in a 10 ml volumetric flask.

Effect of stirring time

To study the effect of stirring time, 1 ml of 100 µg.ml^{-1} Thiocyanate solution was added to 1 ml of 0.1 M Fe (III) solution and 0.5 ml of 0.02 M ammonia buffer and moved to a 10 ml volumetric flask and by adding distilled water brought to volume. Then, each solution was moved to 50 ml bécher containing 0.1 gr of Titanium dioxide nanoparticles and each **bécher was stirre**d for a specific time. Nanoparticles were removed using a filter and the adsorption of each solution was determined by spectrophotometry at $\lambda = 456.8$ nm. Since the removal percentage of Thiocyanate remained constant from the time 15 min, this time was chosen as the optimum time. Fig.4 shows a comparison between the ANN model predictions and the experimental data as a function of contact time.

Effect of the amount of adsorbent

In this regard, 1 ml of 0.1 M Fe (III) solution, 1 ml of 100 µg.ml^{-1} Thiocyanate solution, and 0.5 ml of 0.02 M ammonia buffer were placed in a 10 ml volumetric flask and by adding distilled water brought to volume. Different amounts of Titanium dioxide nanoparticles were placed in 50 ml béchers containing. After 15 min, the solutions were cleared by the filter and the absorption of each solution was determined by spectrophotometry at $\lambda = 456.8$ nm and the optimum amount for Titanium dioxide nanoparticles was 0.5 g. Fig.5 shows a comparison between the ANN model predictions and the experimental data as a function of the amount of adsorbent.

Effect of the volume of Fe(III) solution

To optimize the volume of Fe(III) solution, 1 ml of 100 µg.ml^{-1} Thiocyanate solution and 0.5 ml of ammonia buffer were moved to 10 ml volumetric flasks. Then, different amounts of 0.1 M Iron (III) solution were added to each solution. Next, each solution was brought to volume by adding distilled water, moved to a 50 ml volumetric flask, and placed in contact with 0.5 gr Titanium dioxide nanoparticles. Each solution was stirred for 15 min and cleared by syringe filter. In the final step, the adsorption of each solution was determined by spectrophotometry at $\lambda = 456.8$ nm and 0.01 M Fe (III) was chosen as the optimum amount for the concentration of Fe (III) solution. The agreement between the ANN model predictions and the experimental data as a function of initial volume of Fe (III) is shown in Fig.6.

The effect of the initial concentration of Thiocyanate

To evaluate the effect of the initial concentration of Thiocyanate, different amounts of 1000 gr.ml^{-1} Thiocyanate solution was added to 5 ml of 0.1 M Fe (III) solution, and 2.5 ml of 0.02 M ammonia buffer at pH= 9. Each solution was brought to volume by adding distilled water. Next, each solution was moved to 100 ml béchers containing and placed in contact with 0.5 gr Titanium dioxide nanoparticles. Each solution was stirred for 15 min and cleared by the filter. Then, the adsorption of each solution was determined by spectrophotometry at $\lambda = 456.8$ nm and the optimum concentration of Thiocyanate was 40 µg.ml^{-1}. Fig.7 shows the effect of initial concentration of Thiocyanate on the adsorption
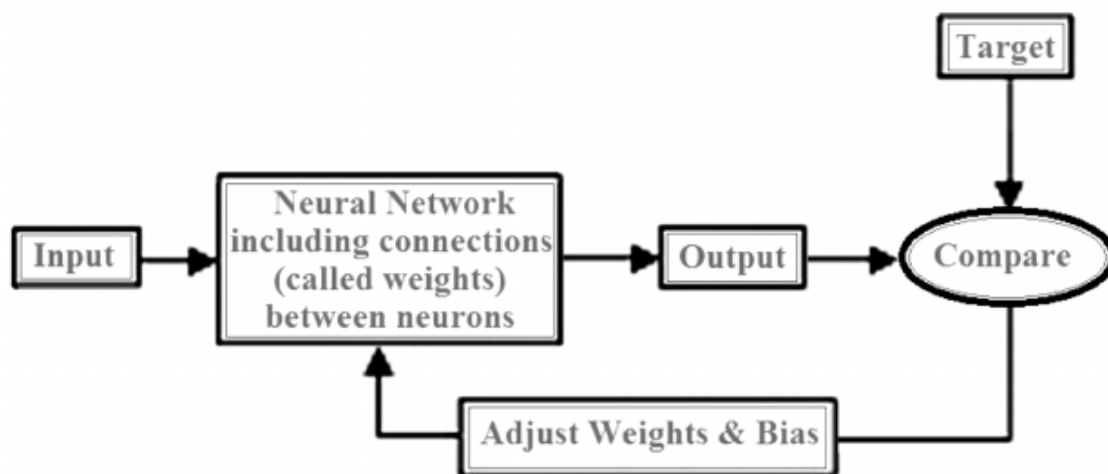
Fig. 1. The schematic of network in the ANN model
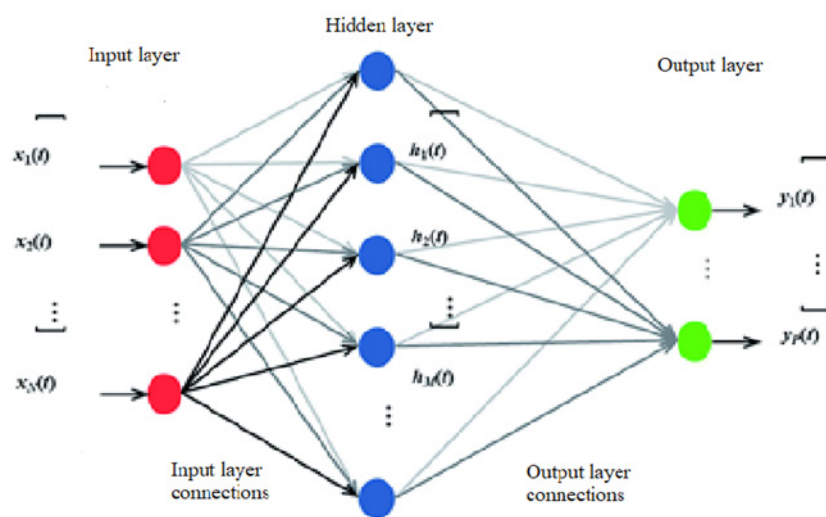
Fig. 2. The schematic of the radial basis function's structure

TABLE 1. Experimental data for training artificial neural network model

N.O	Fe Volume (ml)	TiO$_2$ Concentration (µg.ml^{-1})	Volume (ml)	pH	Adsorbent (g)	Time (min)	R(%)
1	5	10	5	4	0.5	20	50.47
2	5	10	5	5	0.5	20	50.95
3	5	10	5	7	0.5	20	51.31
4	5	10	5	8	0.5	20	51.55
5	5	1	5	9.5	0.5	20	52.06
6	5	1	5	10	0.5	20	51.1
7	1	0.1	1	9	0.1	1	15.3
8	1	0.1	1	9	0.1	2	20.9
9	1	0.1	1	9	0.1	4	29.42
10	1	0.1	1	9	0.1	5	32.36
11	1	0.1	1	9	0.1	7	42.27
12	1	0.1	1	9	0.1	10	47.315
13	1	0.1	1	9	0.1	15	53.89
14	1	0.1	1	9	0.1	17	53.89
15	1	0.1	1	9	0.1	20	83.89
16	1	0.01	1	9	0.5	15	53.98
17	1	0.01	1	9	0.5	15	60.69
18	1	0.01	1	9	0.5	15	89.59
19	1	0.01	1	9	0.5	15	95.92
20	1	0.01	1	9	0.5	15	96.2
21	1	0.01	1	9	0.5	15	96.2
22	0.75	10.0	1	9	0.5	15	94.96
23	1	20.0	1	9	0.5	15	96.25
24	1.5	30.0	1	9	0.5	15	95.11
25	2	40.0	1	9	0.5	15	91.89
26	1	100.0	1	9	0.1	15	53.98
27	1	0.1	1	9	0.2	15	60.69
28	1	0.1	1	9	0.4	15	89.59
29	1	0.1	1	9	0.45	15	95.92
30	1	0.1	1	9	0.6	15	96.2
31	1	0.1	1	9	0.05	15	39.02
32	1	0.1	1	9	0.65	15	96.2

TABLE 2. List of data for test and validation simulated neural network algorithm

N.O	Fe Volume (ml)	TiO$_2$ Concentration ($\mu g.ml^{-1}$)	Volume (ml)	pH	Adsorbent (g)	Time (min)	R(%)
1	5	10	5	6	0.5	20	51.22
2	5	10	5	9	0.5	20	53.05
3	1	0.1	1	9	0.1	3	24.04
4	1	0.1	1	9	0.1	13	50.83
5	1	0.01	1	9	0.5	15	74.6
6	0.5	0.1	1	9	0.5	15	93.05
7	1	0.1	1	9	0.3	15	74.6
8	1	0.1	1	9	0.5	15	96.2
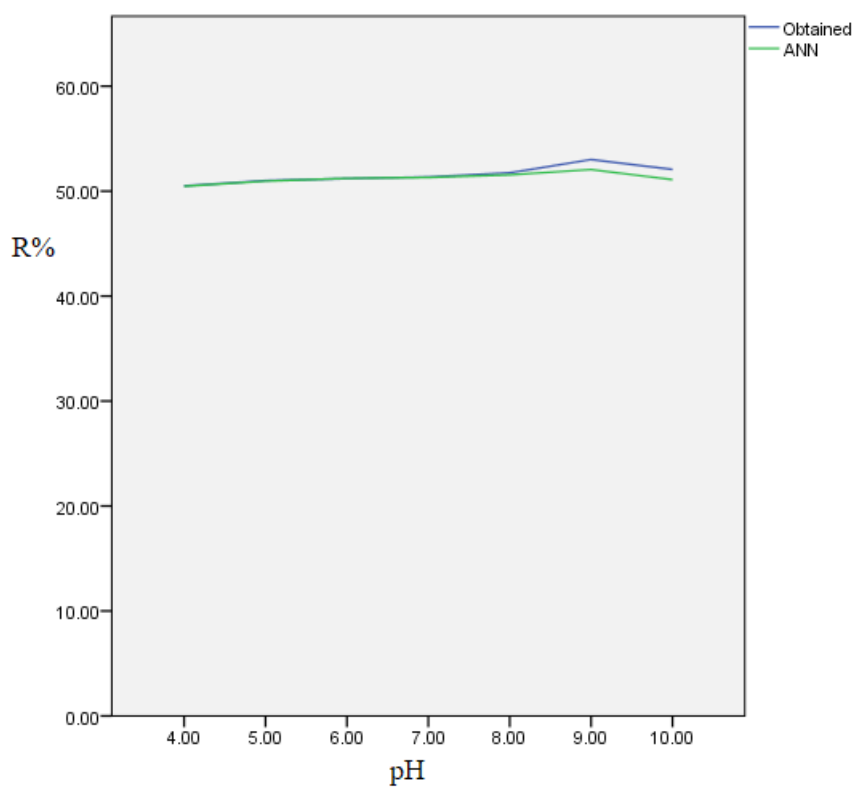
Fig. 3. Agreement between ANN outputs and experimental data as a function of pH
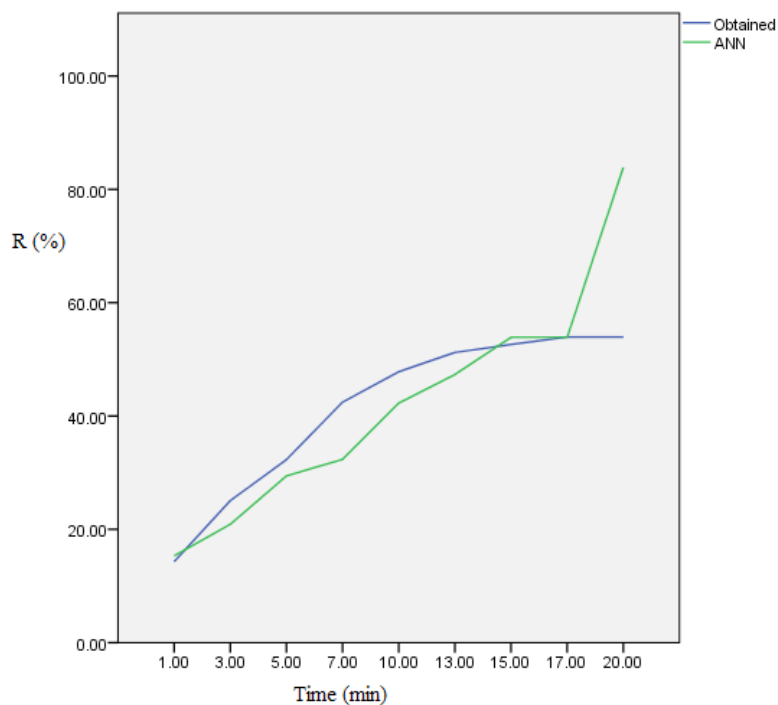
Fig. 4. Agreement between ANN outputs and experimental data as a function of contact time
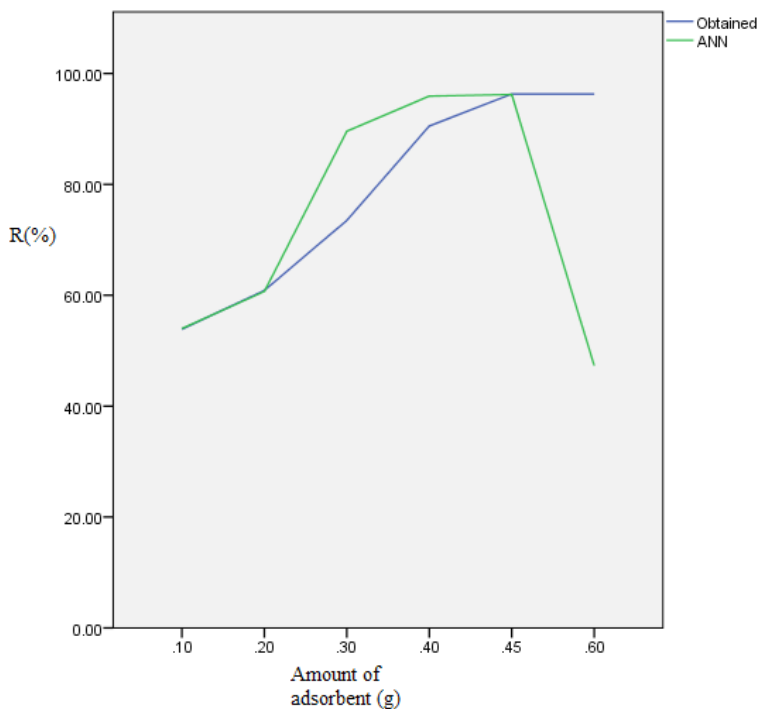
Fig. 5. Agreement between ANN outputs and experimental data as a function of the amount of adsorbent
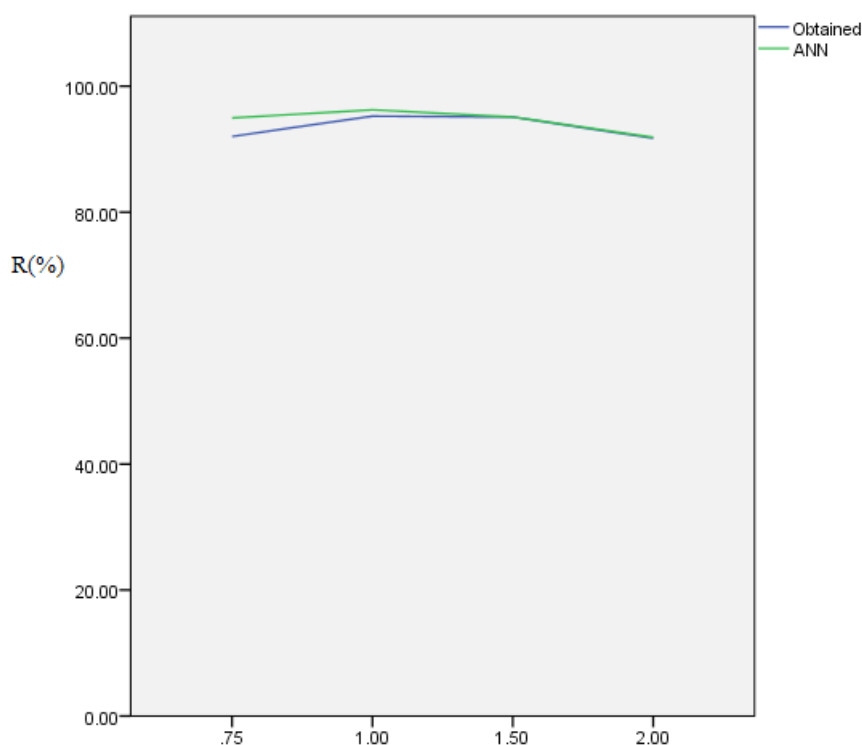
Fig. 6. Agreement between ANN outputs and experimental data as a function of the volume of Fe (III)

process and the agreement between the ANN model predictions and the experimental data.

Statistical diagram of neural network evaluation

Fig. 8 presents the flowchart of the methodology followed in this study. As can be seen, in both methods, the radial basis function and MLP function, training data have lower distribution compared to the testing data. Also, the data deviation from the regression line for MLP, for training data and test data, are smaller than the amount of RBF function, suggesting the better performance of RBF algorithm.

Fig. 9 presents how the actual data obtained from experiments correlate with those predicted by the neural network for training and testing data. As is quite evident, the specifications of the aerodynamic probe can be predicted by the results of the neural network with appropriate accuracy. For both functions, actual and predicted data match together with a high accuracy although the performance of MLP is more appropriate. However, the higher performance of the proposed

algorithm, for predicting the training data compared to test data, is obvious because of making the simulations based on the training data.

The absolute error or the modulus of the difference between the actual and predicted data is presented as a histogram as a dotted line graph (Fig. 10a and 10b) and histogram diagram (Fig. 10c) using the neural network for training and testing data, respectively. During training the neural network by RBF, the maximum absolute error is equal to 1.3954 and its minimum value is 0.1748. Minimum and maximum absolute errors in the training data by MLP function are 0.5031 and 7.48E-07, respectively. Finally, maximum and minimum absolute error for predicting the test data for RBF model and MLP are (4.05 and 0.00882) and (3.405 and 0.2833), respectively.

To determine and examine the detailed performance of functions, neural network efficiency should be evaluated. Statistical parameters were calculated as Equations (5) to (7). The results of the statistical parameters for measuring the performance of MLP and RBF

algorithms are presented in Table 3. As can be seen, for both training and test data, the uncertainty level and mean absolute error for MLP algorithm are closer to zero and the correlation coefficients are closer to one. Hence, the MLP model has a more effective performance in recovery and determination of the amount of the absorbed Thiocyanate [38-40].

$$RMSE = \left[\frac{1}{N} \sum_{i=1}^{N} \left(\hat{u}_i - u_i \right)^2 \right]^{1/2} \qquad \text{Eq. (5)}$$

$$MAE = \frac{1}{N} \sum_{i=1}^{N} \left| \hat{u}_i - u_i \right| \qquad \text{Eq. (6)}$$

$$CE = 1 - \frac{\sum_{i=1}^{N} \left(\hat{u}_i - u_i \right)^2}{\sum_{k=1}^{N} \left(\hat{u}_i - \bar{\hat{u}} \right)^2} \qquad \text{Eq. (7)}$$

Pearson's Chi square

Among feature selection techniques such as Median, Runs, Binomial, Mann-Whitney, Wald-Wolfowiz, Kolmogorov-Smirnov, Sign, Friedman, Wilcoxon, Kruskal Wallis, McNemar, and Cochran Q, the Chi-square test is the most well-known statistics used to test the agreement between observed and theoretical distributions, independency and homogeneity. Furthermore, Pearson's Chi-square is a non-parametric method which can be used for the independent variables. The Chi-square test of independence is used to test statistical independence or association between these two categorical variables. In this case, the statistical question to be answered is what are inter-correlations between variables and output. The null hypothesis for a Chi-square independence test is that two categorical variables are independent. For this purpose, the outputs of all variables were compared and chi square test used to see if there is an association between them. Table 4 shows the case processing summery which presents the number of valid cases used for analysis. Only cases with non-missing values for both the volume of Fe (III) solution (ml) and the volume of Fe (III) solution (ml) can be used in the test [41,42].

Tables 5 and 6 show Fe-Thiocyanate cross-tabulation and chi-square test results, respectively.

The number of degrees of freedom obtained from Equation (8).

df= (R – 1) × (C – 1) Eq. (8)

where R is the number of rows and C is the number of columns. Since the test statistic is based on a 7×2 cross-tabulation table, the degrees of freedom (df) for the test statistic is:

$$df = (R-1) \times (C-1) = (7-1) \times (2-1) = 6$$

The null hypothesis (H_0) and alternative hypothesis (H_1) of the Chi-square test of independence can be expressed in two different but equivalent ways:

H_0: "[Variable 1] is independent of [Variable 2]"

H_1: "[Variable 1] is not independent of [Variable 2]"

OR

H_0: "[Variable 1] is not associated with [Variable 2]"

H_1: "[Variable 1] is associated with [Variable 2]"

The key result in the Chi-square tests table is the Pearson Chi-Square. As can be seen, the amount of Pearson Chi-Square is 29.000. Since there are only 12 cells have expected count less than 5, it seems that these two variables are related significantly. The effect of most variables, including pH*buffer, Fe*buffer, pH*Thiocyanate, Time*Thiocyanate, and Fe*Thiocyanate showed almost the same results. The Pearson Chi-square test for other variables showed more cells have expected count less than 5 which means there are less association between them.

Evaluating real samples

In order to evaluate the performance of the method, some real water samples from the tap water, Karun water, Karkheh dam water, Karun and Fanavaran petrochemicals sewage were prepared. The adsorption capacity ranged from 96.20 to 96.40 mg g^{-1} for tap water, from 95.33 to 96.00 mg g^{-1} for Karun water, from 96.00 to 96.40 mg g^{-1} for o Karkheh dam water, from 95.27 to 96.40 mg g^{-1} for Fanavaran petrochemicals sewage, and from 95.33 to 96.50 mg g^{-1} for Karun petrochemicals sewage. In addition, the adsorption capacity of Thiocyanate was found to be more dependent on pH, time of stirring, and concentration of TiO$_2$. The adsorption capacity increased sharply by enhancing the concentration of TiO$_2$ but it remained constant at the concentration of 0.5 mg
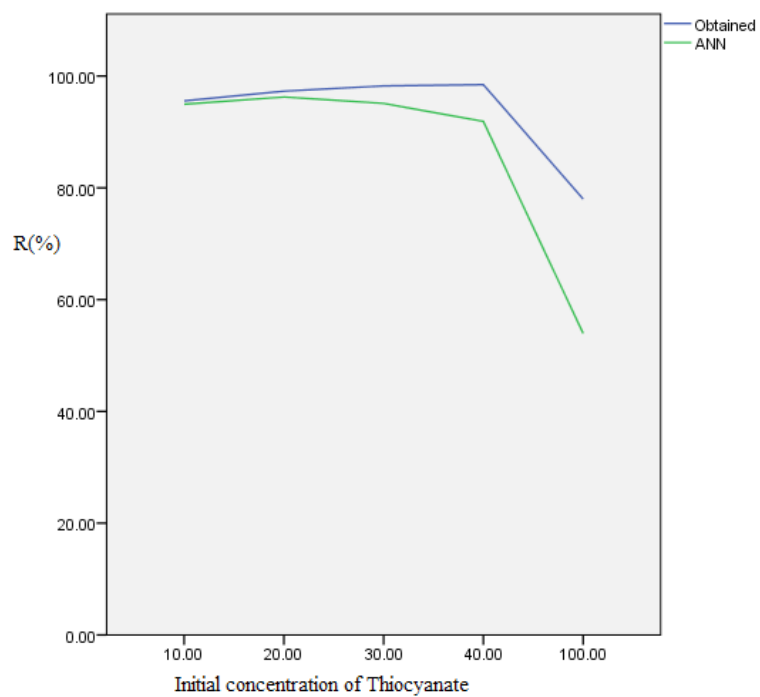
Fig. 7. Agreement between ANN outputs and experimental data as a function of the initial concentration of Thiocyanate
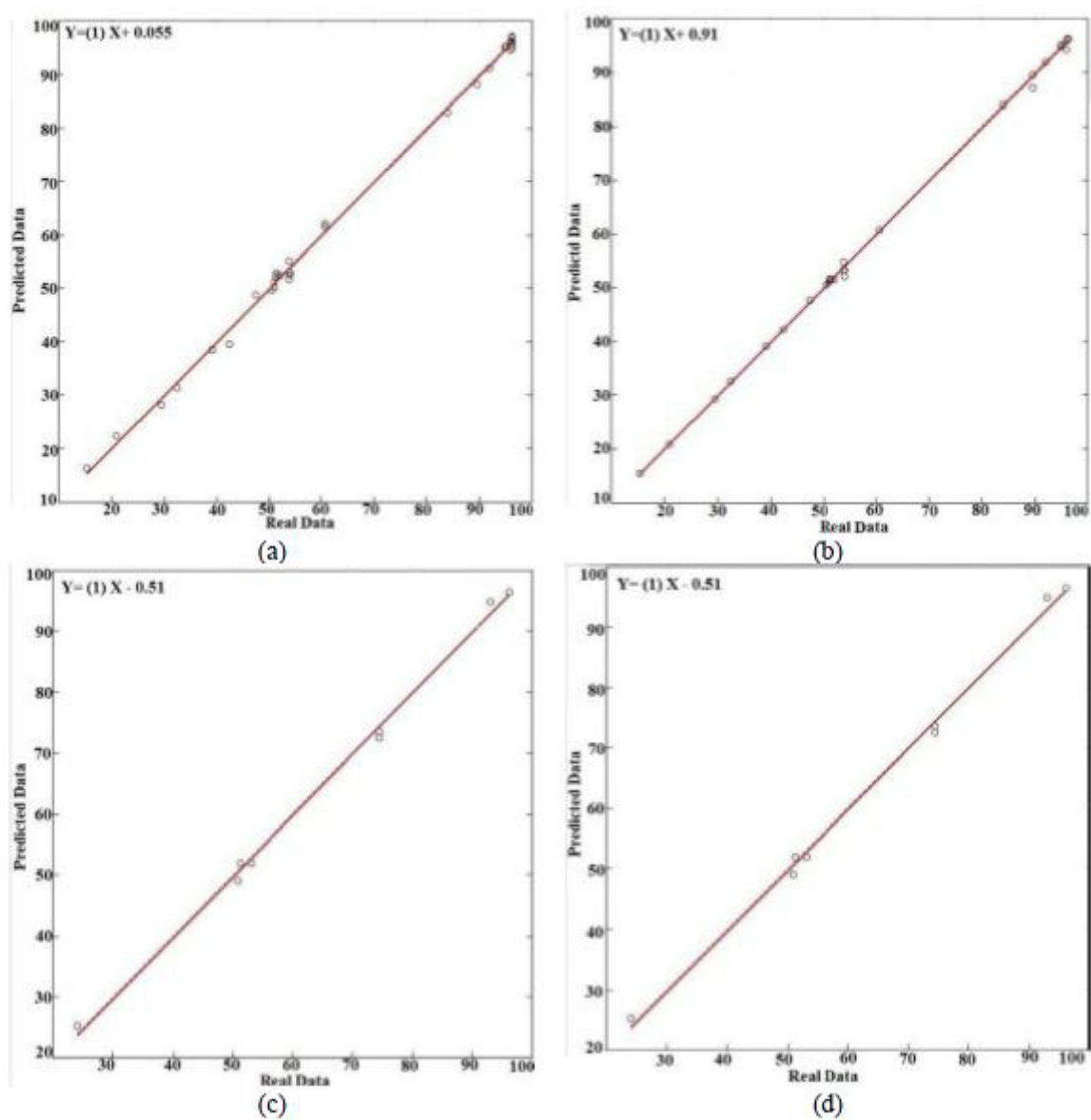
Fig. 8. Regression line for performance of neural network model: radial basis function (a) train data; (c) test data; Levenberg-Marquardt function (b) train data (d) test data
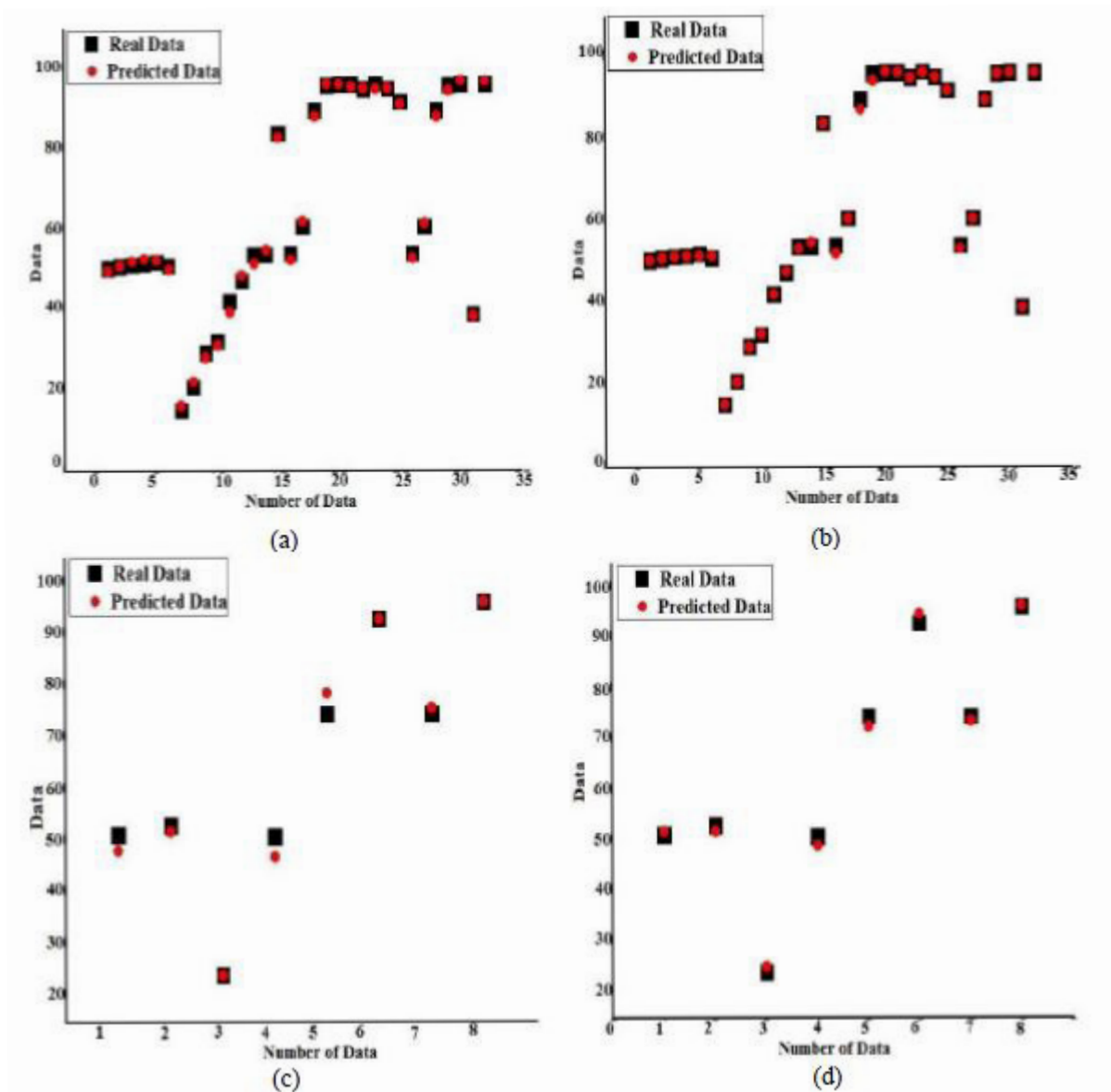
Fig. 9. Point adaption graph of predict and real data: radial basis function (a) train data; (c) test data; Levenberg-Marquardt function (b) train data (d) test data
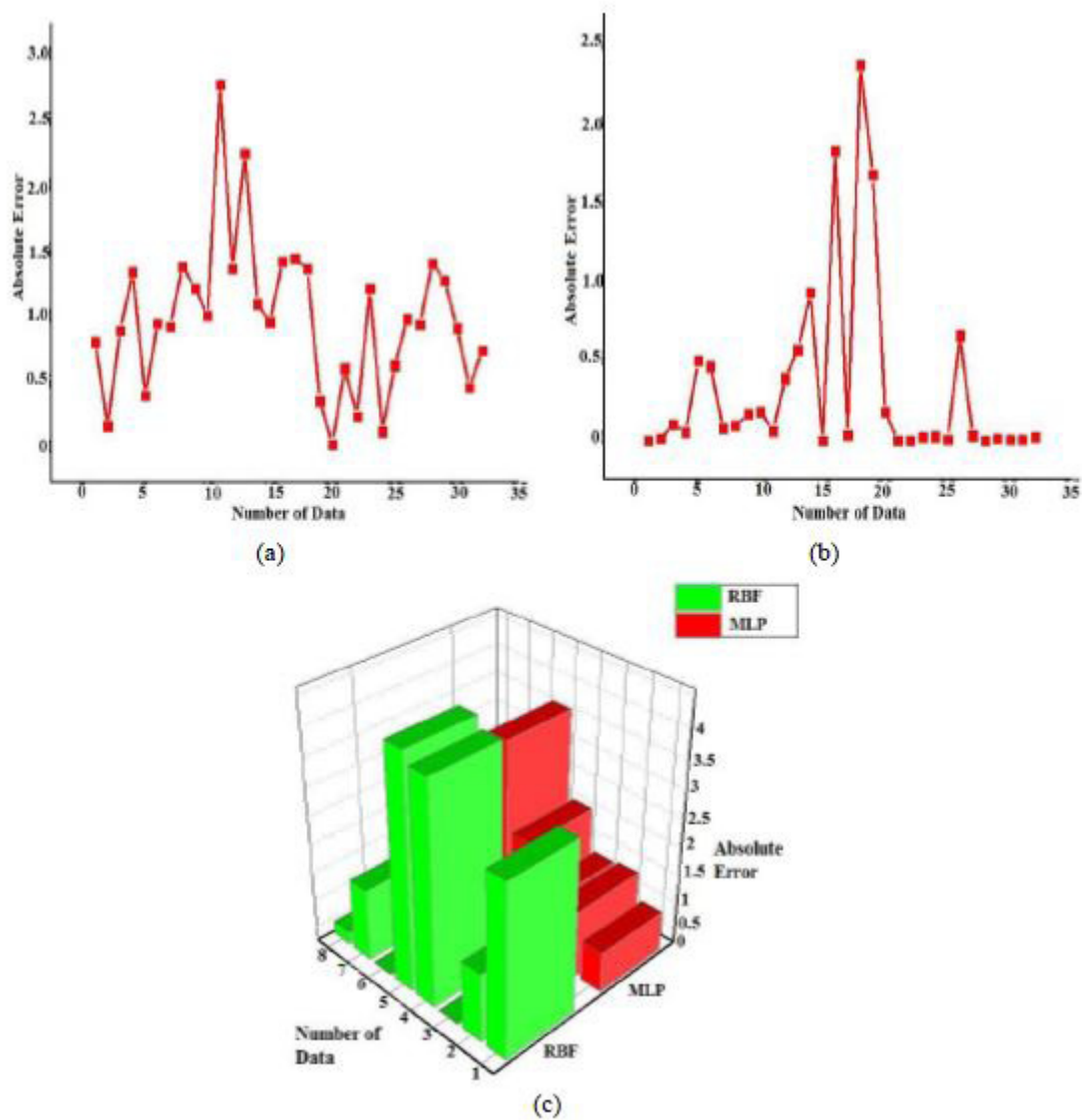
Fig. 10. Absolute error investigation of neural network model: train data (a) radial basis function (b) Levenberg-Marquardt function; (c) test data for radial basis function and Levenberg-Marquardt function

TABLE 3. Statistical parameters for evaluation of efficiency of neural network functions

Function	Algorithm	Statistical parameter		
		Uncertainty	Mean Absolute Error	Coefficient efficiency
Train Data	RBF	1.153537	0.02561875	0.997939
	MLP	0.667157	2.33813E-08	0.99931
Test Data	RBF	2.321255	0.371062	0.990487
	MLP	1.679934	0.087246	0.994627

TABLE 4. Case Processing Summary					
	Cases				
	Valid		Missing		Total	

	N	Percent	N	Percent	N	Percent
Fe * Thiocyanate	20	80.0%	10	20.0%	30	100.0%

TABLE 5. Fe * Thiocyanate Cross-tabulation

Fe * Thiocyanate Cross-tabulation				
				Count
		Thiocyanate		
1.00		5.00		Total
Fe	.01	1	0	1
	.01	1	0	1
	.01	1	0	1
	.15	1	0	1
	.20	1	0	1
	1.00	16	0	16
	5.00	0	8	8
	Total	21	8	29

TABLE 6. The Chi-square test

Chi-Square Tests			
	Value	df	Asymp. Sig. (2-sided)
Pearson Chi-Square	29.000[a]	6	0.001
Likelihood Ratio	34.162	6	0.000
Linear-by-Linear Association	27.133	1	0.002
N of Valid Cases	29		

a. 12 cells (85.7%) have expected count less than 5. The minimum expected count is. 28.

g^{-1}. As demonstrated, time of stirring and pH are important variables in determining Thiocyanate adsorption capacity. Therefore, these variables were chosen, along with the mass of sorbent, volume of solution and volume of Fe (III), to be the input parameters of the computational the artificial neural network models.

Conclusions

In this work, TiO$_2$ nanoparticles were used as an adsorbent and the artificial neural network method was used for simulating the Thiocyanate removal. The vector data were taken at different experimental conditions and, after hard trying, a suitable algorithm was achieved by the effective and widely used neural network functions. The performance of two functions was evaluated by statistical parameters and the results showed that the MLP non-recursive function has a higher ability in the removal of Thiocyanate in comparison with the radial basis function. The advantage of using a neural network in the above method includes reducing the examination time, reducing the costs, and decreasing the use of required laboratory samples.

Acknowledgement

References

1. Ammazzini S., Onor M., Pagliano E., Mester Z., Campanella B., Pitzalis E., Bramanti E. and D'Ulivo A., Determination of thiocyanate in saliva by headspace gas chromatography-mass spectrometry, following a single-step aqueous derivatization with triethyloxonium tetrafluoroborate. *Journal of Chromatography A,* **1400**, 124–130 (2015).

2. Prue D.M., Martin J.E. and Hume A.S., A critical evaluation of thiocyanate as a biochemical index of smoking exposure. *Behavior Therapy,* **11**(3), 368–379 (1980).

3. Afkhami A., Soltani Felehgari F. and Madrakian T., Highly sensitive and selective determination of thiocyanate using gold nanoparticles surface decorated multi-walled carbon nanotubes modified carbon paste electrode. *Sensors and Actuators B: Chemical,* **196**, 467–474 (2014).

4. Nieman R.A. and Anderson D.L., Determination of Iodide and Thiocyanate in powdered milk and in fant formula by online enrichment ion chromatography with photodiode array detection. *Journal of Choromatography A,* **1200**(2), 193-197 (2008).

5. Ahn J.H., Kim J., Lim J. and Hwang, S., Biokinetic evaluation and modeling of continuous Thiocyanate biodegradation by Klebsiella sp. *Biotechnology progress,* **20**(4), 1069-1075 (2004).

6. Scherer G., Carboxyhemoglobin and thiocyanate as biomarkers of exposure to carbon monoxide and hydrogen cyanide in tobacco smoke. *Experimental and Toxicologic Pathology,* **58**(2-3), 101–124 (2006).

7. Baskin S.I., Porter D.W., Rockwood G.A., Romano J.A. J.r., Patel H.C., Kiser R.C., Cook C.M. and Ternay A.L., In vitro and in vivo comparison of sulfur donors as antidote to acute cyanide intoxication. *Journal of Applied Toxicology***,** **19**(3), 173–183 (1999).

8. Baumeister R.G.H., Schievelbein H. and Zickgraf-Rüdel G., Toxicological and clinical aspects of cyanide metabolism. *Arzneimittel-Forschung Drug Research,* **25**(3), 1056–1064 (1975).

9. Wriedt M. and Näther C., Dimorphic modifications of the thiocyanato-bridged coordination polymer [Ni(NCS)$_2$ (pyridazine) (H$_2$O)$_{0.5}$]$_n$ with different magnetic properties. *European Journal of Inorganic Chemistry,* **2011**(2), 228–234 (2011).

10. Logue B.A., Hinkens D.M., Baskin S.I. and Rockwood G.A. The analysis of cyanide and its breakdown products in biological samples. *Critical Reviews in Analytical Chemistry,* **40**(2), 122–147 (2010).

11. Moayyeri N., Saeb K. and Biazar E., Removal of heavy metals (lead, cadmium, zinc,

nickel and iron) from water by bio-ceramic absorbers of hydroxy-apatite microparticles. *International Journal of Marine Science and Engineering,* **3**(1), 13-16 (2013).

12. Cavaco S.A., Fernandes S., Quina M.M. and Ferreira, L.M., Removal of chromium from electroplating industry effluents by ion exchange resins. *Journal of Hazardous Materials,* **144**(3), 634-638 (2007).

13. Erniza M.J.J. and Low S.C., Chromium (III) Removal by Epoxy-Cross-Linked polyether sulfone ultrafiltration membrane. *Jurnal Teknologi (Sciences & Engineering),* **70**(2), 19-22 (2014).

14. Kumari M., PittmanJr Ch.U. and Mohan D., Heavy metals [chromium (VI) and lead (II)] removal from water using mesoporous magnetite (Fe_3O_4) nanospheres. *Journal of Colloid and Interface Science*, **442**, 120-132 (2015).

15. Luo X., Lei X., Xie X., Yu B. and Faquan Yu N.C. Adsorptive removal of Lead from water by the effective and reusable magnetic cellulose nanocomposite beads entrapping activated bentonite. *Carbohydrate Polymers,* **151**, 640-648 (2016).

16. Doke S.M. and Yadav G.D., Process efficacy and novelty of titania membrane prepared by polymeric sol–gel method in removal of chromium (VI) by surfactant enhanced microfiltration. *Chemical Engineering Journal,* **255**, 483-491 (2014).

17. 17. Rajput Sh., PittmanJr Ch.U. and Mohan D., Magnetic magnetite (Fe_3O_4) nanoparticle synthesis and applications for lead (Pb^{2+}) and chromium (Cr^{6+}) removal from water. *Journal of Colloid and Interface Science,* **468**, 334–346 (2016).

18. Karimi H. and Razmara M., Adsorption mechanisms of cadmium onto pillared clays and chalcogenides. *Journal of Sciences, Islamic Republic of Iran,* **23**(3), 231-236 (2012).

19. Sobhanardakani S., Zandipak R., Bonyadi M., Parvizimosaed H., Moslemi M., Tahergorabi R. and Hosseini S.M., Evaluation of removal efficiency of Cr (VI) ions from aqueous solution using Chitosan. *Journal of Chemical Health Risks,* **5**(1), 29-38 (2015).

20. Uheida A., Salazar-Alvarez G., Björkman E., Yu Z. and Muhammed M., Fe_3O_4 and gamma-Fe_2O_3 nanoparticles for the adsorption of Co^{2+} from aqueous solution. *Journal of Colloid and Interface Science,* **298**(2), 501-507 (2006).

21. Nassar N.N., Rapid removal and recovery of Pb(II) from wastewater by magnetic nanoadsorbents. *Journal of Hazardous Materials,* **184**(1-3), 538-546 (2010).

22. Marsh D.H., Jason Riley D., York R.D. and Graydon D., Sopration of inorganic Nano particles in woven cellulose fabrics. *Particuology*, **7**(2), 121-128 (2009).

23. Nabi D., Aslam I. and Qasi I.A. Evaluation of the adsorption potential of titanium dioxide nanoparticles for arsenic removal. *Journal of Environmental Sciences,* **21**(3), 402–408 (2009).

24. Pirilä M., Martikainen M., Ainassaari K., Kuokkanen T. and Keiski R.L., Removal of aqueous As (III) and As (V) by hydrous titanium dioxide. *Journal of Colloid and Interface Science,* **353**(1), 257–262 (2011).

25. HosseiniNia R., Ghaedi M. and Ghaedi A.M., Modeling of reactive orange 12 (RO12) adsorption onto gold nanoparticle-activated carbon using artificial neural network optimization based on an imperialist competitive algorithm. *Journal of Molecular Liquids,* **195**, 219–229 (2014).

26. Ghaedi M., Rozkhoosh Z., Asfaram A., Mirtamizdoust B., Mahmoudi Z. and Bazrafshan A.A., Comparative studies on removal of Erythrosine using ZnS and AgOH nanoparticles loaded on activated carbon as adsorbents: Kinetic and isotherm studies of adsorption. *Spectrochim Acta A Mol Biomol Spectrosc,* **138**, 176–186 (2015).

27. Allahkarami, E., Igder, A., Fazlavi, A., and Rezai, B., Prediction of Co (II) and Ni (II) ions removal from wastewater using artificial neural network and multiple regression models. *Physicochem Problems Miner Processing*, **53**, 1105-1118 (2017).

28. Souza, P. R., Dotto, G. L., and Salau, N. P.

G., Artificial neural network (ANN) and adaptive neuro-fuzzy interference system (ANFIS) modelling for nickel adsorption onto agro-wastes and commercial activated carbon. *Journal of Environmental Chemical Engineering*, **6**(6), 7152-7160 (2018).

29. Özdemir U., Özbay B., Veli S. and Zor S. Modeling adsorption of sodium dodecyl benzene sulfonate (SDBS) onto polyaniline (PANI) by using multi linear regression and artificial neural networks. *Chemical Engineering Journal,* **178**, 183–190 (2011).

30. Fatemi Aghda S.M., Teshnehlab M., Suzuki A., Akiyoshi T. and Kitazono Y., Liquefaction potential assessment using multilayer artificial neural network. *Journal of Sciences, Islamic Republic of Iran,* **9**(3), 245-257 (1998).

31. Maghami P.G. and Sparks D.R., Design of neural networks for fast convergence and accuracy: dynamics and control. *IEEE Transactions Neural Networks,* **11**(1), 113–123 (2000).

32. Khajeh M., Kaykhaii M. and Sharafi A., Application of PSO-artificial neural network and response surface methodology for removal of methylene blue using silver nanoparticles from water samples. *Journal of Industrial and Engineering Chemistry,* **19**(5), 1624–1630 (2013).

33. Mahmoodian H., Moradi O., Shariatzadeha B., Saleh T.A., Tyagi I., Maity A., Asif M. and Gupta V.K., Enhanced removal of methyl orange from aqueous solutions by poly HEMA–chitosan-MWCNT nano-composite. *Journal of Molecular Liquids,* **202**, 189–198 (2015).

34. 34. Kong C., Wang H., Li D., Zhang Y., Pan J., Zhu B. and Luo Y. Quality changes and predictive models of radial basis function neural networks for brined common carp (Cyprinus carpio) fillets during frozen storage. *Food Chemistry,* **201**, 327–333 (2016).

35. Haykin S. Neural Networks: A Comprehensive Foundation, 2nd ed. Chap. 1, Hamilton, Ontario, Canada, 34-38 (1998).

36. Haykin S. Neural Networks and Learning Machines, 3rd ed. Chap. 5, Hamilton, Ontario, Canada, 239-242 (2008).

37. Ranganathan A. The Levenberg-Marquardt Algorithm, Honda Research Institute, Ohio, USA, (2004). http://www.ananth.in/Notes_files/lmtut.pdf

38. 38. Mustafa M.R., Rezaur R.B., Rahardjo H. and Isa M.H., Prediction of pore-water pressure using radial basis function neural network. *Engineering Geology,* **135-136**, 40-47 (2012).

39. Bulut, A., Yusan, S., Aytas, S., Sert, S., and Akpolat, O., Artificial Neural Network (ANN) Approach for Modeling of Sr (II) Adsorption from Aqueous Solution by Natural Calcium-based Materials. *Research Journal of Environmental Sciences*, **12**, 121-131 (2018).

40. Agatonovic-Kustrin, S., and Beresford, R., Basic concepts of artificial neural network (ANN) modeling and its application in pharmaceutical research. *Journal of Pharmaceutical and Biomedical Analysis,* **22**, 712-722 (2000).

41. Paokanta, P., β-Thalassemia knowledge elicitation using data engineering: PCA, Pearson's chi square and machine learning. *International Journal of Computer Theory and Engineering*, **4**, 702-706 (2012).

42. Bolboacă, S.D., Jäntschi, L., Sestraş, A.F., Sestraş, R.E., and Pamfil, D.C., Pearson-Fisher chi-square statistic revisited. *Information*, **2,** 528-545 (2011).

التنبؤ بكمية إزالة أنيونات الثيوسيانات المائية بواسطة جسيمات ثاني أكسيد التيتانيوم النانوية

باستخدام طرق الشبكة العصبية الاصطناعية الحديثة

راشين اندايش*،'، مهران زرگران'

' قسم الكيمياء ، فرع العلوم والبحوث ، جامعة آزاد الإسلامية ، الأهواز ، إيران

²قسم الكيمياء ، جامعة آزاد الإسلامية في الأحواز ، الأهواز ، إيران

في هذا التحقيق ، يتم تنفيذ طريقة الامتصاص باستخدام نمذجة الشبكة العصبية (ANN) يتم تطبيق المادة الماصة لإزالة ثيوسيانات في عينات المياه باستخدام جزيئات ثاني أكسيد التيتانيوم (TiO_2) كمادة ماصة فعالة. تم التحقيق في كمية التنبؤ لإزالة الثيوسيانات مع خوارزميات جديدة للشبكة العصبية. لهذا الغرض، تم اختيار ستة معلمات كبيانات إدخال التدريب لوظائف الشبكة العصبية بما في ذلك الرقم الهيدروجيني ، ووقت التحريك ، وكتلة المواد الماصة والحجم وتركيز TiO_2 ، وحجم (III) Fe. تم فحص أداء الطرق المقترحة باستخدام معلمات إحصائية ووجد أنها مخرجات فعالة وفعالة للنمذجة.